Weak-and strong-coupling limits of the two-dimensional Fröhlich polaron with spin-orbit Rashba interaction

C. Grimaldi
Max-Planck-Institut für Physik komplexer Systeme, Nöthnitzer Strasse 38, D-01187 Dresden, Germany and LPM, Ecole Polytechnique Fédérale de Lausanne, Station 17, CH-1015 Lausanne, Switzerland
(Received 21 September 2007; published 15 January 2008)

The continuous progress in fabricating low-dimensional systems with large spin-orbit couplings has reached a point in which nowadays materials may display spin-orbit splitting energies ranging from a few to hundreds of meV. This situation calls for a better understanding of the interplay between the spin-orbit coupling and other interactions ubiquitously present in solids, in particular when the spin-orbit splitting is comparable in magnitude with characteristic energy scales such as the Fermi energy and the phonon frequency. In this article, the two-dimensional Fröhlich electron-phonon problem is reformulated by introducing the coupling to a spin-orbit Rashba potential, allowing for a description of the spin-orbit effects on the electron-phonon interaction. The ground state of the resulting Fröhlich-Rashba polaron is studied in the weak and strong-coupling limits of the electron-phonon interaction for arbitrary values of the spin-orbit splitting. The weak-coupling case is studied within the Rayleigh-Schrödinger perturbation theory, while the strong-coupling electron-phonon regime is investigated by means of variational polaron wave functions in the adiabatic limit. It is found that, for both weak- and strong-coupling polarons, the ground-state energy is systematically lowered by the spin-orbit interaction, indicating that the polaronic character is strengthened by the Rashba coupling. It is also shown that, consistently with the lowering of the ground state, the polaron effective mass is enhanced compared to the zero spin-orbit limit. Finally, it is argued that the crossover between weakly and strongly coupled polarons can be shifted by the spin-orbit interaction.

DOI: 10.1103/PhysRevB.77.024306 PACS number(s): 71.38.−k, 71.38.Fp, 71.70.Ej

I. INTRODUCTION

The Fröhlich Hamiltonian describing a single electron coupled to longitudinal optical phonons is a paradigmatic model of the electron-phonon (el-ph) interaction,[1] and has represented in the past, in addition to its interest for the solid-state physics, an ideal problem for testing many mathematical methods in quantum field theory.[2] Because of the coupling with the phonon field, the resulting quasiparticle, the polaron, has an effective mass larger, and a ground-state energy lower than the free electron. These quantities have been investigated for the three-dimensional (3D) case by means of perturbation theory for the weak-coupling limit,[3] and of variational treatments for the intermediate-[4] and strong-coupling cases.[5,6] The path-integral variational calculations of Feynman,[7] and subsequent refinements of this method,[8] have provided a solid description for all values of the coupling, verified also by improved variational methods,[9] and by quantum Monte Carlo studies.[10,11]

The interest aroused some time ago on semiconductor heterojunctions, or other low-dimensional systems, prompted to modify the Fröhlich model to accounting for two-dimensional (2D) and quasi-2D systems.[12] By applying the same methods derived for the 3D case, the ground-state properties for the strictly 2D case were evaluated for weak, strong, and intermediate couplings,[13–16] and the obtained systematic lowering of the ground-state energy and the enhancing of the effective mass compared to the 3D case has pointed out the role of dimensionality in enhancing the polaronic character.[12,17]

Concerning the el-ph problem in low dimensions, recent progresses in developing high-quality low-dimensional systems and in material engineering provide hints that, for a vast class of low-dimensional materials, the usual 2D Fröhlich model, as considered in literature, may be incomplete. This concern comes about by considering 2D systems exhibiting strong spin-orbit (SO) splitting of the electronic states due to the inversion asymmetry in the direction orthogonal to the conducting plane (Rashba SO mechanism). This situation is encountered in semiconductor quantum wells with asymmetric confining potentials,[18] in the surface states of metals and semimetals,[19–21] and in surface alloys such as Li/W(110),[22] Pb/Ag(111),[23,24] and Bi/Ag(111),[25] with SO splitting energies ranging from a few meV in GaAs quantum wells to about 0.2 eV in Bi/Ag(111).[25] In these systems, therefore, the SO energy may be of the same order or even much larger than the typical phonon frequency, rising the question of how such state of affair affects the el-ph interaction, in general, and the Fröhlich coupling, in particular.

As pointed out in several works,[26–31] the Rashba interaction describing the SO coupling can have profound effects on the low-energy properties of the itinerant electrons. Namely, in the low-density regime, the Rashba SO coupling induces a topological change of the Fermi surface of the free electrons, leading to an effective reduction of the dimensionality in the electronic density of states (DOS). In this situation, a 2D low density electron gas would develop, in the presence of SO Rashba coupling, a phenomenology similar to one-dimensional (1D) systems, triggered by the square-root divergence of the (effectively 1D) DOS at low energies.

Some interesting consequences of this scenario on the el-ph problem have already been discussed in Ref. 30, concerning the superconducting transition, and in Ref. 31 for the effective mass and the spectral properties. The picture arising

from these works, although being limited to the momentum-independent Holstein el-ph interaction and to weak-to-moderate couplings, confirms that, for sufficiently low electron densities, the coupling to the phonons is amplified by the SO interaction through the 1D-like divergence of the DOS.

Notwithstanding the relevance of these results for the Holstein model, the use of a local el-ph interaction may, however, result inadequate in the extremely low electron density regime, where the SO effects are more evident.[30,31] Indeed, the lack of effective screening in this case would rather suggest a long-range interaction as being a more appropriate description of the el-ph coupling. It is therefore natural to consider the 2D Fröhlich polaron, and its coupling to the SO interaction, as a model better describing the unscreened el-ph interaction in 2D Rashba systems in the low density limit.

In this article, a single electron moving with a parabolic dispersion in the two-dimensional x-y plane is coupled simultaneously to the Rashba SO potential and to the phonon degrees of freedom through a Fröhlich interaction term. The total system is then described by the 2D Fröhlich-Rashba Hamiltonian $H=H_{\mathrm{el}}+H_{\mathrm{ph}}+H_{\mathrm{el\text{-}ph}}$, where ($\hbar=1$)

$$H_{\mathrm{el}}=\frac{p^2}{2m}+\mathbf{\Omega}(\mathbf{p})\cdot\boldsymbol{\sigma} \tag{1}$$

is the Hamiltonian for an electron with mass m and momentum operator $\mathbf{p}=-i\boldsymbol{\nabla}$ with components $(p_x,p_y,0)$, $\boldsymbol{\sigma}$ is the spin-vector operator with components given by the Pauli matrices, and $\mathbf{\Omega}(\mathbf{p})$ is the SO vector field which in the case of Rashba coupling reduces to

$$\mathbf{\Omega}(\mathbf{p})=\gamma\begin{pmatrix}-p_y\\ p_x\\ 0\end{pmatrix}, \tag{2}$$

where γ is the SO coupling parameter. The phonon part of the Hamiltonian is given by

$$H_{\mathrm{ph}}=\omega_0\sum_{\mathbf{q}}a_{\mathbf{q}}^{\dagger}a_{\mathbf{q}}, \tag{3}$$

where $a_{\mathbf{q}}^{\dagger}$ ($a_{\mathbf{q}}$) is the creation (annihilation) operator for a phonon with momentum $\mathbf{q}=(q_x,q_y)$ and optical frequency ω_0. The el-ph interaction Hamiltonian for the 2D electron coupled to longitudinal optical (LO) phonons is[12,14]

$$H_{\mathrm{el\text{-}ph}}=\frac{1}{\sqrt{A}}\sum_{\mathbf{q}}\frac{1}{\sqrt{q}}(M_0e^{i\mathbf{q}\cdot\mathbf{r}}a_{\mathbf{q}}+M_0^{*}e^{-i\mathbf{q}\cdot\mathbf{r}}a_{\mathbf{q}}^{\dagger}) \tag{4}$$

with

$$M_0=i\omega_0\left(\frac{2\pi^2\alpha^2}{m\omega_0}\right)^{1/4}, \tag{5}$$

where $\alpha=e^2(\epsilon_{\infty}^{-1}-\epsilon_0^{-1})\sqrt{m/2\omega_0}$ is the dimensionless el-ph coupling constant, with e being the electron charge, and ϵ_{∞} and ϵ_0 the high frequency and static dielectric constants, respectively.

It is worth clarifying here the significance of the 2D Fröhlich interaction of Eq. (4) with respect to the characteristics of specific materials. For quantum wells and 2D heterostructures, where the electron wave function is assumed here to be confined in a sheet of zero thickness, Eq. (4) describes the coupling of the electron to bulk LO phonons, while the coupling to interface phonon modes is neglected. The inclusion of such interface phonon contributions may be important in describing specific materials, but it is unnecessary for the present study, where the focus is on the SO effects on the unscreened (long-range) el-ph interaction, for which Eq. (4) is a paradigm for the 2D case. Concerning the el-ph coupling of electronic surface states, Eq. (4) coincides (apart from a redefinition of M_0) with the coupling to 2D surface phonons when the coupling to bulk phonons extending below the surface is negligible.[32] Such approximation is coherent with the ideal 2D assumption for the electron wave function, which is physically realized when the electronic surface states have negligible coupling to the bulk. A further motivation of using the 2D Fröhlich model (4) is that, in the absence of SO interaction, the ground-state polaron energy E_P and effective mass m^* have already been studied by several authors,[12–16] and the exact results obtained for the weak- ($\alpha\ll1$) and strong- ($\alpha\gg1$) coupling limits provide a useful reference for the effect of nonzero SO coupling.

In the present work, the 2D Fröhlich-Rashba Hamiltonian is studied by considering the weak- and strong-coupling limits of the el-ph interaction, with arbitrary strength of the SO coupling γ. For $\alpha\ll1$ the polaron energy E_P and the effective mass m^* are obtained from second order perturbation theory in Sec. II, where numerical and exact analytical results are presented. It is shown that the effect of $\gamma\neq0$ is qualitatively similar to that observed in the Holstein model,[30,31] namely, the SO coupling enhances the effective coupling to the phonons. In particular, E_P is lowered by γ and, simultaneously, the effective mass m^* is enhanced. In Sec. III the strong-coupling limit $\alpha\gg1$ is treated by the variational method, providing a rigorous upper bound of the ground state energy for arbitrary values of the SO interaction. As for the weak el-ph coupling case, it is found that E_P (m^*) is lowered (enhanced) by the SO interaction, implying that the Rashba coupling always amplifies the polaronic character, regardless of whether the el-ph interaction is weak or strong.

II. WEAK COUPLING

In the presence of SO interaction, the electron wave function is a spinor and its Green's function is conveniently represented by a 2×2 matrix in the spin subspace. For $\alpha=0$ the free electron Green's function $\mathbf{G}_0$ is readily obtained from H_{el}:

$$\mathbf{G}_0(\mathbf{k},\omega)=\left(\omega-\frac{k^2}{2m}-\mathbf{\Omega}(\mathbf{k})\cdot\boldsymbol{\sigma}\right)^{-1}$$
$$=\frac{1}{2}\sum_{s=\pm}[1+s\hat{\mathbf{\Omega}}(\mathbf{k})\cdot\boldsymbol{\sigma}]G_0^{s}(k,\omega), \tag{6}$$

where $\mathbf{k}$ is a 2D electron wave number $\hat{\mathbf{\Omega}}(\mathbf{k})=\mathbf{\Omega}(\mathbf{k})/|\mathbf{\Omega}(\mathbf{k})|$ and

$$G_0^s(k,\omega) = \frac{1}{\omega - k^2/2m - s\gamma k} \tag{7}$$

is the free electron propagator for the two ($s=\pm 1$) chiral states characterized by two distinct bands with shifted parabolic dispersions $k^2/2m \pm \gamma k$. The lowest band has its minimum value $-E_0$ at $k=k_0$, where k_0 and E_0 are the Rashba momentum and energy defined, respectively, by

$$k_0 = m\gamma, \quad E_0 = \frac{m}{2}\gamma^2. \tag{8}$$

For later convenience, it is useful to express the electron energy relative to E_0, so that the poles of Eq. (7) appear at energies

$$E_\pm(k) = \frac{1}{2m}(k \pm k_0)^2. \tag{9}$$

The free electron ground state is then given by the electron occupying the lower band at wave number $k=k_0$ with energy $\omega=0$.

In the weak el-ph coupling limit ($\alpha \ll 1$) the ground-state properties are obtained by the electron self-energy evaluated in the second order perturbation theory. At zero temperature, the resulting single electron self-energy is therefore

$$\mathbf{\Sigma}(\mathbf{k},\omega) = |M_0|^2 \int \frac{d\mathbf{k}'}{(2\pi)^2} \frac{1}{|\mathbf{k}-\mathbf{k}'|} \mathbf{G}_0(\mathbf{k}', \omega - \omega_0). \tag{10}$$

Because of the momentum dependence of the Fröhlich interaction, and contrary to the Holstein el-ph case considered in Ref. 31, the self-energy is not diagonal in the spin subspace. However, since the momentum dependence enter only through the modulus of the momentum transfer, Eq. (10) can be rewritten in a quite simple form. By using $[\hat{\mathbf{\Omega}}(\mathbf{k})\cdot\boldsymbol{\sigma}]^2 = 1$ and

$$[\hat{\mathbf{\Omega}}(\mathbf{k})\cdot\boldsymbol{\sigma}][\hat{\mathbf{\Omega}}(\mathbf{k}')\cdot\boldsymbol{\sigma}] = \hat{\mathbf{k}}\cdot\hat{\mathbf{k}}' + (\hat{\mathbf{k}}\times\hat{\mathbf{k}}')\sigma_x\sigma_y, \tag{11}$$

then the quantity $\hat{\mathbf{\Omega}}(\mathbf{k}')\cdot\boldsymbol{\sigma}$ appearing in Eq. (10) through $\mathbf{G}_0(\mathbf{k}', \omega-\omega_0)$ can be replaced simply by $[\hat{\mathbf{\Omega}}(\mathbf{k})\cdot\boldsymbol{\sigma}]\hat{\mathbf{k}}\cdot\hat{\mathbf{k}}'$ because the second term of Eq. (11) vanishes after the integration over $\mathbf{k}'$. In this way, the resulting self-energy reduces to

$$\mathbf{\Sigma}(\mathbf{k},\omega) = \mathbf{\Sigma}_d(k,\omega)\mathbf{1} + \Sigma_o(k,\omega)\hat{\mathbf{\Omega}}(\mathbf{k})\cdot\boldsymbol{\sigma}, \tag{12}$$

where $\mathbf{1}$ is the unit matrix and Σ_d and Σ_o are, respectively, the diagonal and off-diagonal contributions to the self-energy, both depending solely on the modulus of $\mathbf{k}$.[33] Their explicit expressions are

$$\mathbf{\Sigma}_d(k,\omega) = \frac{|M_0|^2}{2} \int \frac{d\mathbf{k}'}{(2\pi)^2} \sum_s \frac{1}{|\mathbf{k}-\mathbf{k}'|} \frac{1}{\omega - \omega_0 - E_s(k')}, \tag{13}$$

$$\mathbf{\Sigma}_o(k,\omega) = \frac{|M_0|^2}{2} \int \frac{d\mathbf{k}'}{(2\pi)^2} \sum_s \frac{1}{|\mathbf{k}-\mathbf{k}'|} \frac{s\mathbf{k}\cdot\mathbf{k}'}{\omega - \omega_0 - E_s(k')}. \tag{14}$$

In the limit of zero SO coupling, since $E_s(k) \to k^2/2m$, $\Sigma_o(k,\omega)$ vanishes because of the summation over $s=\pm 1$ in Eq. (14). Notice also that, independently of γ, $\Sigma_o(k,\omega)=0$ when the factor $1/|\mathbf{k}-\mathbf{k}'|$ in Eq. (14) is replaced by a constant, as in the momentum-independent Holstein el-ph coupling model.

By using Eq. (12) the Dyson equation for the interacting propagator $\mathbf{G}$ reduces to

$$\begin{aligned}\mathbf{G}^{-1}(\mathbf{k},\omega) &= \mathbf{G}_0^{-1}(\mathbf{k},\omega) - \mathbf{\Sigma}(\mathbf{k},\omega) \\ &= \omega - \frac{k^2}{2m} - \Sigma_d(k,\omega) - E_0 \\ &\quad - [\gamma k + \Sigma_o(k,\omega)]\hat{\mathbf{\Omega}}(\mathbf{k})\cdot\boldsymbol{\sigma},\end{aligned} \tag{15}$$

and the poles $\omega_\pm$ of $\mathbf{G}$ are then given by

$$\omega_\pm = E_\pm(k) + \Sigma_d(k,\omega_\pm) \pm \Sigma_o(k,\omega_\pm). \tag{16}$$

Now, the Rayleigh-Schrödinger perturbation theory permits us to evaluate the lower-energy pole ω_- at the lowest order in the el-ph coupling α. This is accomplished by replacing ω_- by the unperturbed energy $E_-(k)$ in the energy variables of Σ_d and Σ_o. In this way, the lower pole reduces to $\omega_- = E_-(k) + \Sigma_-(k) + O(\alpha^2)$, where

$$\Sigma_-(k) = \Sigma_d[k, E_-(k)] - \Sigma_o[k, E_-(k)]. \tag{17}$$

Finally, by expanding $\Sigma_-(k)$ up to the second order in $k-k_0$, the polaron dispersion in the vicinity of k_0 can be written as

$$\omega_- = E_P + \frac{1}{2m^*}(k - k_0^*)^2, \tag{18}$$

where the polaron ground-state energy E_P, the effective mass m^*, and the effective Rashba momentum k_0^* are given, respectively, by

$$E_P = \Sigma_-(k_0) - \frac{m^*}{2}\Sigma_-'(k_0)^2 = \Sigma_-(k_0) + O(\alpha^2), \tag{19}$$

$$\frac{m^*}{m} = [1 + m\Sigma_-''(k_0)]^{-1} = 1 - m\Sigma_-''(k_0) + O(\alpha^2), \tag{20}$$

$$\frac{k_0^*}{k_0} = 1 - \frac{m^*}{k_0}\Sigma_-'(k_0) = 1 - \frac{m}{k_0}\Sigma_-'(k_0) + O(\alpha^2). \tag{21}$$

Let us first consider E_P and m^*. In the zero SO limit, Eqs. (19) and (20) at $k_0=0$ lead, respectively, to $E_P = \pi\alpha\omega_0/2$ and $m^*/m = 1 + \pi\alpha/8$, which correspond to the results already reported in Refs. 13–15. For finite values of the SO coupling the ground-state energy and the effective mass can be expressed as

$$E_P = -\frac{\pi}{2}\alpha\omega_0 f_{E_P}(\varepsilon_0), \tag{22}$$

$$\frac{m^*}{m} = 1 + \frac{\pi}{8}\alpha f_{m^*}(\varepsilon_0), \tag{23}$$

where the factors $f_{E_P}(\varepsilon_0)$ and $f_{m^*}(\varepsilon_0)$ contain all the effects of the SO interaction and depend solely on the dimensionless SO parameter

$$\varepsilon_0 \equiv \frac{E_0}{\omega_0} = \frac{m\gamma^2}{2\omega_0}. \tag{24}$$

In the weak SO limit, the self-energy terms (13) and (14) can be expanded in powers of the SO interaction, allowing for an analytical evaluation of the integrals. In this way, up to the linear order in ε_0, $f_{E_P}(\varepsilon_0)$, and $f_{m^*}(\varepsilon_0)$ are found to be

$$f_{E_P}(\varepsilon_0) = 1 + \frac{\varepsilon_0}{4} + O(\varepsilon_0^2), \tag{25}$$

$$f_{m^*}(\varepsilon_0) = 1 + \frac{9}{8}\varepsilon_0 + O(\varepsilon_0^2), \tag{26}$$

indicating that the polaronic character is strengthened by the SO interaction since, through Eqs. (22) and (23), the polaron energy E_P is lowered and, simultaneously, the effective mass m^* is enhanced when $\varepsilon_0 > 0$. This feature is not limited to the small ε_0 limit, but holds true for arbitrary strengths of the SO coupling. This is shown in Fig. 1, where $f_{E_P}(\varepsilon_0)$ and $f_{m^*}(\varepsilon_0)$, obtained from a numerical integration of Eqs. (13) and (14), are plotted as a function of ε_0 by solid lines and compared with Eqs. (25) and (26) (dashed lines). The same quantities calculated for a wider range of ε_0 are plotted in the insets of Fig. 1 and confirm that the ground-state energy E_P and the effective mass m^* are continuous functions of ε_0 and are, respectively, further lowered and enhanced by the SO coupling. In the strong SO limit $\varepsilon_0 \gg 1$, it is found that $f_{E_P}(\varepsilon_0)$grows as $\ln(\varepsilon_0)$ while $f_{m^*}(\varepsilon_0)$ grows linearly. It is interesting to note that the Holstein-Rashba model studied in Ref. 31 predicts results qualitatively similar to the Fröhlich model, indicating that the SO interaction strengthen the polaronic character independently of the specific form of the el-ph interaction.[34]

In addition to E_P and m^*, the interplay between the el-ph coupling and the SO interaction modifies also the Rashba momentum k_0 through Eq. (21). In the weak SO limit, the effective quantity k_0^* is found to be

$$\frac{k_0^*}{k_0} \simeq 1 - \frac{\pi}{32}\alpha\varepsilon_0, \tag{27}$$

indicating a reduction of the bare Rashba momentum k_0, confirmed also by the numerical calculation of Eq. (21) reported in Fig. 2 by the solid line. As shown in the inset, for fixed el-ph coupling α, k_0^*, however, does not deviate much from its bare limit k_0, even for large values of the SO parameter ε_0.

Let us compare now the present results with those appeared recently in literature. In Ref. 35 the ground-state energy of a polaron near a polar-polar semiconductor interface with Rashba SO coupling has been evaluated with the Lee-Low-Pines method.[4] As a function of the SO splitting, the polaron ground state is found to be lowered, in qualitative agreement therefore with the present results. A more quantitative comparison is however precluded by the different model of Ref. 35, where contributions from interface phonon modes and confining potentials are considered as well. In another work,[36] the Rayleigh-Schrödinger perturbation

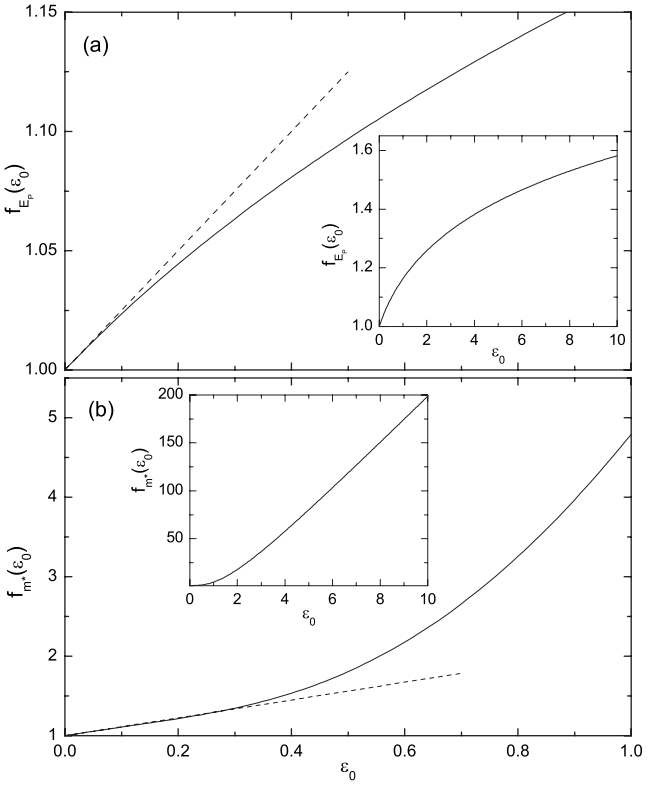

FIG. 1. (a) Ground-state energy factor $f_{E_P}(\varepsilon)$ as a function of the SO parameter $\varepsilon_0 = E_0/\omega_0$. The solid line is the numerical calculation, while the dashed line is the weak SO limit Eq. (25). Inset: $f_{E_P}(\varepsilon)$ plotted for a wider range of ε_0. (b) The effective mass factor $f_{m^*}(\varepsilon_0)$ from numerical integration (solid line) and from Eq. (26) (dashed line). Inset: $f_{m^*}(\varepsilon_0)$ plotted for a wider range of ε_0.

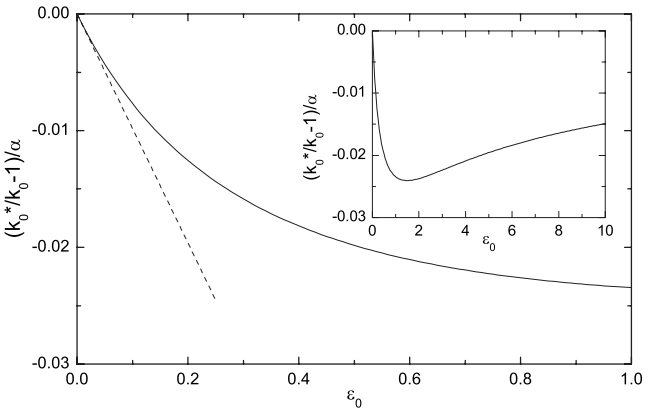

FIG. 2. Effective Rashba momentum k_0^* as a function of the SO parameter $\varepsilon_0 = E_0/\omega_0$. The numerical integration of Eq. (21) (solid line) is compared with the weak SO result (27) (dashed line). Inset: the same quantity plotted for a wider range of ε_0.

theory has been applied to the polaron ground state of the 2D Fröhlich-Rashba model, permitting therefore a direct comparison with the analysis presented here. Despite that the authors of Ref. 36 find that the polaron ground state is lowered by ε_0, their values of E_P differ from those plotted in Fig. 1(a). In Ref. 36, in fact, the ground-state energy factor f_{E_P} is found to be $f_{E_P}(\varepsilon_0)=1/\sqrt{1-\varepsilon_0}$, which implies a small ε_0 expansion different from Eq. (25) and, more importantly, a divergence of E_P at $\varepsilon_0=1$. In Fig. 1(a), instead, nothing of special happens at $\varepsilon_0=1$. This discrepancy is easily traced back in the fact that in Ref.36 the expansion of $\Sigma_-(k)$, Eq. (17), is made around $k=0$, instead of $k=k_0$ as done here, which does not correspond to a perturbative calculation of the ground-state energy.

The results presented in this section have been derived by assuming a weak coupling to the phonons. However, as it is clear from the plots in Fig. 1, the enhancement of the polaronic character driven by ε_0 for fixed α unavoidably renders the perturbative approach invalid for sufficiently large ε_0 values. For example, from Eq. (23), the validity of the weak-coupling results for m^*/m are subjected to the condition $\alpha f_{m^*}(\varepsilon_0)\ll 1$, otherwise higher order el-ph contributions should be considered for a consistent description of the SO effects. The question remains therefore whether the SO enhancement of the polaronic character survives also for large α values, or it is instead limited to the weak-coupling limit. In the next section, this problem is studied for the limiting case of strong el-ph interaction $\alpha\gg 1$, providing therefore, together with the weak-coupling results, a global understanding of the SO effects on the Fröhlich polaron.

III. STRONG COUPLING

It is well known that a perturbative scheme such that employed in the previous section fails to describe the Fröhlich polaron ground state when the el-ph coupling is very large. This is due to the fact that for $\alpha\gg 1$ the lattice polarization, and resulting "self-trapping" effect experienced by the electron,[37] renders the plane wave representation of the unperturbed electron inappropriate for obtaining the polaron ground state. Instead, as originally proposed in Ref. 5 and rigorously proved in Refs. 38 and 39, the asymptotic description of the polaron wave function in the strong-coupling limit $\alpha\gg 1$ is that of a product between purely electronic $\psi(\mathbf{r})$ and purely phononic $|\xi\rangle$ wave functions. Within such an adiabatic limit, the ground-state energy and the effective mass of a 2D Fröhlich polaron have been calculated in Refs. 14 and 15 by using the variational method with different *Ansatz* wave functions. From Ref. 14, one realizes that exponential, Gaussian, and Pekar-type wave functions provide increasingly better estimates of E_P with accuracies, respectively, of 14, 0.3, and 0.03 % with respect to the exact ground-state energy $E_P/\omega_0=-0.40474\alpha^2$, obtained by a numerical solution of the integrodifferential equation for the electron wave function.[16] In the following, the variational method is used to evaluate the SO effects on the polaron ground state.

A. Trial wave functions

For the nonzero SO case, due to the presence of the Pauli matrices in Eq. (1), suitable *Ansatz* wave functions must take into account the electron spin degrees of freedom. Hence, in full generality, the strong-coupling polaron wave function may be represented as $|\mathbf{\Psi},\xi\rangle=\mathbf{\Psi}(\mathbf{r})|\xi\rangle$, where $\mathbf{\Psi}(\mathbf{r})$ is a two-component spinor for the electron. The corresponding expectation value of the total Hamiltonian H is

$$\langle\mathbf{\Psi},\xi|H\mathbf{\Psi},\xi=\langle\mathbf{\Psi}|H_{\rm el}|\mathbf{\Psi}\rangle+\langle\xi|H_{\rm ph}|\xi\rangle + \frac{1}{\sqrt{A}}\sum_{\mathbf{q}}\frac{1}{\sqrt{q}}[M_0\rho(\mathbf{q})\langle\xi|a_{\mathbf{q}}|\xi\rangle+\text{H.c.}], \tag{28}$$

where

$$\rho(\mathbf{q})=\langle\mathbf{\Psi}|e^{i\mathbf{q}\cdot\mathbf{r}}|\mathbf{\Psi}\rangle=\int d\mathbf{r}e^{i\mathbf{q}\cdot\mathbf{r}}|\mathbf{\Psi}(\mathbf{r})|^2. \tag{29}$$

The form of Eq. (28) permits to integrate out the phonon wave function in the usual way. Hence, by introducing the phonon coherent state $|\xi\rangle=\mathcal{N}e^{\Sigma_{\mathbf{q}}\xi_{\mathbf{q}}a_{\mathbf{q}}^\dagger}|0\rangle$, where $\mathcal{N}$ is a normalization factor and $\xi_{\mathbf{q}}$ a variational parameter, minimization of Eq. (28) with respect to $\xi_{\mathbf{q}}$ leads to the functional

$$E[\mathbf{\Psi}]=\langle\mathbf{\Psi}|H_{\rm el}|\mathbf{\Psi}\rangle-\frac{|M_0|^2}{\omega_0}\int\frac{d\mathbf{q}}{(2\pi)^2}\frac{1}{q}|\rho(\mathbf{q})|^2, \tag{30}$$

where the continuum limit $A^{-1}\Sigma_{\mathbf{q}}\to\int d\mathbf{q}/(2\pi)^2$ has been performed. By choosing an appropriate functional form for $\mathbf{\Psi}(\mathbf{r})$, and by minimizing $E[\mathbf{\Psi}]$ with respect to the variational parameters defining $\mathbf{\Psi}(\mathbf{r})$, an upper bound for the ground-state energy is then $E[\mathbf{\Psi}_0]$, where $\mathbf{\Psi}_0(\mathbf{r})$ is such that $E[\mathbf{\Psi}_0]=\min(E[\mathbf{\Psi}])$. As done in the previous section, the polaron energy is then obtained from

$$E_P=E[\mathbf{\Psi}_0]+E_0, \tag{31}$$

where E_0 is the free-electron SO energy defined in Eq. (8).

Of course, the functional form of $\mathbf{\Psi}(\mathbf{r})$ is decisive for obtaining accurate estimates of the ground-state energy, and a suitable choice must be guided by looking at the properties of the true ground-state spinor $\mathbf{\Psi}_G(\mathbf{r})$. These can be deduced by a formal minimization of the functional $E[\mathbf{\Psi}]$ with respect to $\mathbf{\Psi}$. By introducing the Lagrange multiplier ϵ to ensure that the wave function is normalized to unity, minimization of Eq. (30) leads to

$$H_{\rm el}\mathbf{\Psi}(\mathbf{r})+V(\mathbf{r})\mathbf{\Psi}(\mathbf{r})=\epsilon\mathbf{\Psi}(\mathbf{r}), \tag{32}$$

where, by using the definition of $\rho(\mathbf{q})$ given in Eq. (29):

$$V(\mathbf{r})=-\frac{2|M_0|^2}{\omega_0}\int\frac{d\mathbf{q}}{(2\pi)^2}\frac{\rho(\mathbf{q})^*}{q}e^{i\mathbf{q}\cdot\mathbf{r}} =-\frac{|M_0|^2}{\pi\omega_0}\int d\mathbf{r}'\frac{|\mathbf{\Psi}(\mathbf{r}')|^2}{|\mathbf{r}-\mathbf{r}'|}. \tag{33}$$

From the above expression of $V(\mathbf{r})$, the functional (30) can be rewritten as $E[\mathbf{\Psi}]=\langle\mathbf{\Psi}|H_{\rm el}|\mathbf{\Psi}\rangle+\bar{V}/2$, where $\bar{V}=\langle\mathbf{\Psi}|V(\mathbf{r})|\mathbf{\Psi}\rangle$. Now, if $\mathbf{\Psi}_G$ is the exact ground-state wave function, with ground-state energy $E_G=E[\mathbf{\Psi}_G]$, then, from Eq. (32) and $E_G=\langle\mathbf{\Psi}|H_{\rm el}|\mathbf{\Psi}\rangle+\bar{V}/2$, it is found that $\epsilon=E_G+\bar{V}/2$, so that Eq. (32) reduces to

$$H_{\mathrm{el}}\mathbf{\Psi}_G(\mathbf{r}) + [V(\mathbf{r}) - \bar{V}/2]\mathbf{\Psi}_G(\mathbf{r}) = E_G\mathbf{\Psi}_G(\mathbf{r}). \quad (34)$$

As noted in Ref. 29 (see also Refs. 40 and 41), the ground-state wave function of a 2D electron subjected to a SO Rashba interaction and to a 2D central potential (i.e., a potential depending only upon $r=|\mathbf{r}|$) is of the form

$$\mathbf{\Psi}_G(\mathbf{r}) = \begin{pmatrix} \psi_1(r) \\ \psi_2(r)e^{i\varphi} \end{pmatrix}, \quad (35)$$

where φ is the azimuthal angle of $\mathbf{r}$. Now, if Eq. (35) is used in Eq. (33), the resulting self-consistent potential depends only upon r, $V(\mathbf{r}) \to V(r)$, so that Eq. (35) is consistently also the correct form for the polaron ground-state wave function. Hence, passing to polar coordinates, Eq. (34) can be rewritten as a system of integrodifferential equations for the spinor components ψ_1 and ψ_2:

$$\left[-\frac{1}{2m}\left(\frac{d^2}{dr^2} + \frac{1}{r}\frac{d}{dr}\right) + U(r)\right]\psi_1(r) - \gamma\left(\frac{d}{dr} + \frac{1}{r}\right)\psi_2(r) = E_G\psi_1(r), \quad (36)$$

$$\left[-\frac{1}{2m}\left(\frac{d^2}{dr^2} + \frac{1}{r}\frac{d}{dr} - \frac{1}{r^2}\right) + U(r)\right]\psi_2(r) + \gamma\frac{d}{dr}\psi_1(r) = E_G\psi_2(r), \quad (37)$$

where $U(r)=V(r)-\bar{V}/2$ and the polaron energy is obtained from $E_P=E_G+E_0$. By introducing the dimensionless variable $\rho=r/l_P$, where $l_P=1/\alpha(m\omega_0)^{1/2}$ is a measure of the polaron spatial extension in the zero SO limit, and by noticing that E_G does not depend on the sign of γ, it is straightforward to realize from Eqs. (36) and (37) that the polaron ground-state energy scales as

$$E_P = \mathcal{F}\left(\frac{\varepsilon_0}{\alpha^2}\right)\alpha^2\omega_0, \quad (38)$$

where $\varepsilon_0=E_0/\omega_0$ is the dimensionless SO energy introduced in Eq. (24) and $\mathcal{F}$ is a generic function. It is found therefore from Eq. (38) that the dependence of E_P on the SO interaction is through the effective parameter ε_0/α^2, which is treated in the following as an independent variable. Although ε_0/α^2 is then formally allowed to vary from 0 to ∞, it is nevertheless important to estimate the range over which ε_0/α^2 is expected to vary for reasonable values of the microscopic parameters E_0, ω_0, and α. To this end, it must be reminded that the strong-coupling limit of a 2D Fröhlich polaron (in the absence of SO interaction) is appropriate only for $\alpha \gtrapprox 5$,[12] and that the typical phonon energy scale is of the order of few to tens meV, say $\omega_0 \approx 5-10$ meV. The largest value of the Rashba energy E_0 reported so far is of about 0.2 eV,[25] so that $\varepsilon_0/\alpha^2 \lesssim 1-2$ is a rather conservative estimate compatible with material parameters and with the strong-coupling polaron hypothesis.

Let us now evaluate the behavior of $\psi_1(r)$ and $\psi_2(r)$ for $r \ll l_P$ and $r \gg l_P$. By requiring a regular solution at the origin, it turns out by inspection of Eqs. (36) and (37) that the spinor components of Eq. (35) behave as $\psi_1(r)=$const and $\psi_1(r) \propto r$ as $r \to 0$, while the behavior for $r \gg l_P$ is obtained from the large r limit of Eqs. (36) and (37):

$$-\frac{1}{2m}\frac{d^2\psi_1(r)}{dr^2} - \gamma\frac{d\psi_2(r)}{dr} = W\psi_1(r), \quad (39)$$

$$-\frac{1}{2m}\frac{d^2\psi_2(r)}{dr^2} + \gamma\frac{d\psi_1(r)}{dr} = W\psi_2(r), \quad (40)$$

where the quantity $W=E_G+\bar{V}/2$ is negative for bound states. Solutions of Eqs. (39) and (40) which are finite for $r \to \infty$ are linear combination of $\exp(-\lambda_+ r)$ and $\exp(-\lambda_- r)$ with

$$\lambda_\pm = \sqrt{-2m(E_P + \bar{V}/2)} \pm ik_0, \quad (41)$$

implying an exponential decay of the polaron wave function, accompanied by periodic oscillations of wavelength $2\pi/k_0$.

The informations gathered on the limiting behaviors of the ground state wave function are sufficient for guessing some appropriate trial wave functions to be used in Eq. (30). By assuming that for zero SO coupling the electron is in a spin-up state, then a simple *Ansatz* compatible with the limits discussed above is

$$\mathbf{\Psi}(\mathbf{r}) = f(r)\begin{pmatrix} \cos(br) \\ \sin(br)e^{i\varphi} \end{pmatrix}, \quad (42)$$

where b is a variational SO parameter vanishing for $\gamma=0$ and $f(r)$ is an exponentially decaying function for $r \to \infty$ and such that $f(0) \neq 0$. The advantage of Eq. (42) is that one can use exponential or Pekar-type functions for $f(r)$, automatically recovering therefore the known results for the zero SO case.[14] It should be noted, however, that in the $U(r) \to 0$ limit Eq. (42) does not reproduce correctly the behavior of the exact ground-state wave function, which is instead given by Eq. (35) with $\psi_1(r)$ and $\psi_2(r)$ proportional to the Bessel functions $J_0(k_0 r)$ and $J_1(k_0 r)$, respectively.[40,41] Hence, Eq. (42) is not expected to provide a reliable ground-state energy in the strong SO regime, for which $U(r)$ can be treated as a perturbation. To remedy to this deficiency, the following alternative form of the polaron *Ansatz* is proposed:

$$\mathbf{\Psi}(\mathbf{r}) = f(r)\begin{pmatrix} J_0(br) \\ J_1(br)e^{i\varphi} \end{pmatrix}, \quad (43)$$

where, as before, b is a variational SO parameter. As it will be shown below, the lowest value of E_P is given either by Eq. (42) or by Eq. (43), depending on the specific form considered for $f(r)$ and on the value of the SO coupling.

B. Ground-state energy

To evaluate the polaron ground-state energy, three different trial wave functions for $f(r)$ are considered: exponential, Gaussian, and Pekar type. As shown below, the Gaussian *Ansatz* will provide results comparable to those coming from the exponential and Pekar functions, despite its faster decay for $r \to \infty$ compared to Eq. (41). These three trial wave functions will be used in combination with the sinuisodal and the

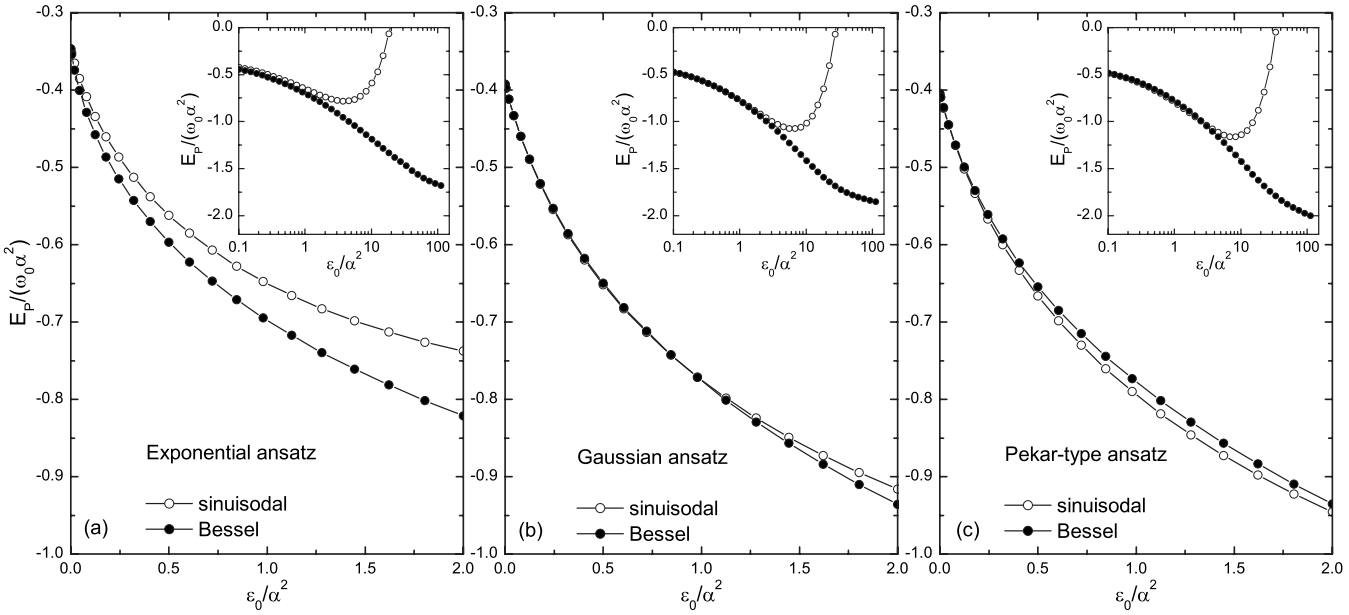

FIG. 3. Polaron ground-state energy as a function of ε_0/α^2 for different trial wave functions for $f(r)$. (a) Exponential, (b) Gaussian, (c) Pekar. The sinuisodal and the Bessel type of *Ansätze* are given, respectively, by Eq. (42) and Eq. (43). Inset: the polaron energy for a wider range of ε_0/α^2 values.

Bessel-type spinors of Eqs. (42) and (43), respectively, giving a total of six different *Ansätze* for the Fröhlich-Rashba polaron wave function.

Exponential Ansatz. Let us start by evaluating the functional $E[\Psi]$, Eq. (30), by using the exponential *Ansatz* $f(r)=\mathcal{A}\exp(-ar)$, where a is a variational parameter and $\mathcal{A}$ is a normalization factor, in combination with the sinuisodal trial wave function (42). By introducing the dimensionless quantities $\tilde{a}=al_P$, $\tilde{b}=bl_P$, and $\tilde{\gamma}=k_0l_P$, for nonzero SO interaction the functional (30) evaluated with the exponential-sinuisodal *Ansatz* reduces to

$$\frac{E[\Psi]}{\alpha^2\omega_0}=\frac{1}{2}\left[\tilde{a}^2+\tilde{b}^2+\tilde{a}^2\ln\left(1+\frac{\tilde{b}^2}{\tilde{a}^2}\right)\right]-\tilde{\gamma}\tilde{b}\left(1+\frac{\tilde{a}^2}{\tilde{a}^2+\tilde{b}^2}\right)-\frac{3\pi\tilde{a}}{8\sqrt{2}}. \tag{44}$$

For weak SO couplings, Eq. (44) has its minimum at $\tilde{b}=\tilde{\gamma}=\sqrt{2\varepsilon_0}/\alpha$ and $\tilde{a}=3\sqrt{2}\pi/16$, so that the resulting polaron energy $E_P=E[\Psi_0]+E_0$ becomes

$$\frac{E_P}{\alpha^2\omega_0}=-\left(\frac{3\pi}{16}\right)^2-\frac{\varepsilon_0}{\alpha^2}+O\left(\frac{\varepsilon_0^2}{\alpha^4}\right). \tag{45}$$

In the $\varepsilon_0=0$ limit, Eq. (45) reduces to $E_P/\alpha^2\omega_0=-(3\pi/16)^2\simeq-0.3469$, recovering therefore the result of Ref. 14, while for $\varepsilon_0>0$ the polaron energy is lowered by the SO interaction, in qualitative analogy with the weak electron-phonon behavior discussed in Sec. II. The lowering of E_P is confirmed by a numerical minimization of Eq. (44) whose results are plotted in Fig. 3(a) (open circles). For $\varepsilon_0/\alpha^2=1$, the polaron energy has dropped to $E_P/\alpha^2\omega_0\simeq-0.65$, which is about two times lower than the zero SO case. However, upon increasing ε_0/α^2, E_P displays a minimum at $\varepsilon_0/\alpha^2\simeq3.98$ [inset of Fig. 3(a)] and for larger values of the SO interaction the polaron energy increases. Eventually, for $\varepsilon_0/\alpha^2\gtrsim14$ the calculated ground-state energy becomes larger than the zero SO value $E_P/\alpha^2\omega_0=-(3\pi/16)^2$. Such upturn of E_P for large ε_0 stems from the inadequacy of the sinuisodal components of Eq. (42) in treating the oscillatory behavior in the strong SO regime which, as pointed out above, should instead be given by Bessel-type functions. Indeed when the exponential *Ansatz* for $f(r)$ is used in Eq. (43), rather than in Eq. (42), not only is the resulting E_P lower than the previous case, but also the upturn of E_P disappears, leading to a monotonous lowering of the polaron energy as ε_0/α^2 increases [filled circles in Fig. 3(a)]. As $\varepsilon_0/\alpha^2\to\infty$, however, the polaron energy does not decrease indefinitely but rather approaches a limiting value. Although an accurate numerical evaluation of E_P for $\varepsilon_0/\alpha^2>100$ has turned out to be difficult, the asymptotic value of E_P can nevertheless be obtained analytically from the strong SO limit of the exponential-Bessel expression for $E[\Psi]$:

$$\frac{E[\Psi]}{\alpha^2\omega_0}=\frac{\tilde{a}^2+\tilde{b}^2}{2}-\tilde{b}\tilde{\gamma}-\frac{\pi}{\sqrt{2}}\tilde{a}, \tag{46}$$

whose minimum is at $\tilde{b}=\tilde{\gamma}$ and $\tilde{a}=\pi/\sqrt{2}$, leading to

$$\lim_{\varepsilon_0/\alpha^2\to\infty}\frac{E_P}{\alpha^2\omega_0}=-\frac{\pi^2}{4}\simeq-2.467. \tag{47}$$

Gaussian Ansatz. The results obtained by using a Gaussian wave function of the form $f(r)=\mathcal{A}\exp(-a^2r^2)$ are plotted in Fig. 3(b). Compared to the exponential wave function, the Gaussian *Ansatz* gives an overall lowering of the polaron energy for both sinuisodal and Bessel forms of the spinors.

In the $\varepsilon_0/\alpha^2 \ll 1$ limit, and independently of which particular spinor is used, the ground-state polaron energy is found to be

$$\frac{E_P}{\alpha^2\omega_0} = -\frac{\pi}{8} - \frac{\varepsilon_0}{\alpha^2} + O\left(\frac{\varepsilon_0^2}{\alpha^4}\right), \tag{48}$$

confirming in this regime the linear dependence on the SO coupling of Eq. (45). For larger values of the SO coupling, and contrary to the case shown in Fig. 3(a), the sinuisodal and Bessel-type spinors give basically the same values of E_P for all SO couplings up to $\varepsilon_0/\alpha^2 \simeq 1$. Beyond this value, as for the case with the exponential wave function, the polaron energy obtained from the sinuisodal *Ansatz* becomes larger than that obtained from the Bessel spinor and, as shown in the inset of Fig. 3(b), rapidly increases while the Gaussian-Bessel ansatz gives a monotonous lowering of E_P. For $\varepsilon_0/\alpha^2 \gg 1$, the Gaussian-Bessel energy functional has the same form of Eq. (46) with the latter term substituted by $-2.279\tilde{a}$, which implies

$$\lim_{\varepsilon_0/\alpha^2\to\infty} \frac{E_P}{\alpha^2\omega_0} \simeq -2.579. \tag{49}$$

Pekar-type Ansatz. Let us now evaluate E_P by using in Eqs. (42) and (43) the Pekar-type *Ansatz* $f(r)=\mathcal{A}(1+a_1 r+a_2 r^2)\exp(-ar)$. For zero SO coupling, this *Ansatz* gives $E_P/\alpha^2\omega_0 \simeq -0.4046$,[14] which is a lower energy than those obtained from the exponential and Gaussian trial wave functions and only 0.03% higher than the exact result −0.40474 of Ref. 16. As shown in Fig. 3(c), the Pekar-type *Ansatz* gives slightly better estimates of E_P also for nonzero SO couplings, with an overall behavior similar to the previous cases. Namely, in the weak SO regime one finds

$$\frac{E_P}{\alpha^2\omega_0} = -0.4046 - \frac{\varepsilon_0}{\alpha^2} + O\left(\frac{\varepsilon_0^2}{\alpha^4}\right) \tag{50}$$

and, as before, for stronger SO couplings the energy obtained from the sinuisodal spinor increases indefinitely with ε_0/α^2. However, contrary to the exponential and Gaussian *Ansätze*, the Pekar-type wave function may give a lower polaron energy when used in combination with the sinuisodal spinor. This holds true as long as $\varepsilon_0/\alpha^2 \lesssim 2.72$, while for stronger SO couplings it is the Bessel-type spinor which gives the lower E_P [inset of Fig. 3(c)]. A numerical minimization of the asymptotic limit of the Pekar-Bessel functional for $\varepsilon_0/\alpha^2 \gg 1$ gives

$$\lim_{\varepsilon_0/\alpha^2\to\infty} \frac{E_P}{\alpha^2\omega_0} \simeq -2.91, \tag{51}$$

which is lower than the asymptotic values of Eqs. (47) and (49).

The results plotted in Fig. 3 clearly demonstrate that, since the variational method provides an upper bound for true ground-state polaron energy, the lowering of E_P induced by the SO coupling is a robust feature of the strong-coupling Fröhlich-Rashba polaron. Among the different *Ansätze* studied, the lower polaron energy is obtained by using a Pekar-type wave function for $f(r)$ in combination with the sinuisodal spinor for weak to moderate values of ε_0/α^2 or with the Bessel-type spinor for stronger SO couplings. Given that, as discussed above, reasonable values of ε_0/α^2 for strongly coupled polarons fall in the range $0 \leq \varepsilon_0/\alpha^2 \lesssim 1-2$, the Pekar-sinuisodal wave function provides therefore the best description of the Fröhlich-Rashba polaron in this regime.

C. Effective mass

As demonstrated in Sec. II, the effective mass m^* of a weakly coupled polaron is enhanced by the SO interaction and, given the results above, the same phenomenon is reasonably expected to occur also for the strong-coupling case. To quantify the polaron mass enhancement within the localized wave function formalism, it is useful to follow the approach of Refs. 42–44, briefly described below, where a moving wave packet is constructed from the localized wave function. The quantity to minimize is

$$J_{\boldsymbol{v}}[\Psi',\xi'] = \langle \Psi',\xi'|H - \boldsymbol{v}\cdot\mathbf{P}|\Psi',\xi'\rangle, \tag{52}$$

where $\boldsymbol{v}$ is a Lagrange multiplier, which will turn out to be the mean polaron velocity, and $\mathbf{p}=\mathbf{p}+\Sigma_{\mathbf{q}}\mathbf{q}a_{\mathbf{q}}^{\dagger}a_{\mathbf{q}}$ is the total momentum operator. The wave function $|\Psi',\xi'\rangle$ is given by the product $\Psi'(\mathbf{r})|\xi'\rangle$, where

$$\Psi'(\mathbf{r}) = e^{i\mathbf{p}_0\cdot\mathbf{r}}\Psi(\mathbf{r}) \tag{53}$$

is the electron wave packet with $\mathbf{p}_0$ being a variational momentum, $\Psi(\mathbf{r})$ is the *Ansatz* localized wave function, and $|\xi'\rangle = \mathcal{N}e^{\Sigma_{\mathbf{q}}\xi'_{\mathbf{q}}a_{\mathbf{q}}^{\dagger}}|0\rangle$. Minimization of Eq. (52) with respect to $\xi'_{\mathbf{q}}$ gives now the functional

$$J_{\boldsymbol{v}}[\Psi'] = \langle\Psi'|H_{\mathrm{el}} - \boldsymbol{v}\cdot\mathbf{p}|\Psi'\rangle - |M_0|^2\int\frac{d\mathbf{q}}{(2\pi)^2}\frac{|\rho(\mathbf{q})'|^2}{q}\frac{1}{\omega_0 - \mathbf{q}\cdot\langle\Psi'|\boldsymbol{v}|\Psi'\rangle}, \tag{54}$$

where $\mathbf{p}$ is the electron momentum operator and $\rho(\mathbf{q})' = \langle\Psi'|e^{i\mathbf{q}\cdot\mathbf{r}}|\Psi'\rangle$. By using Eq. (53), it is easily shown that $J_{\boldsymbol{v}}[\Psi']$ reduces to

$$J_{\boldsymbol{v}}[\Psi'] = \langle\Psi|H_{\mathrm{el}}|\Psi\rangle + \frac{p_0^2}{2m} - \mathbf{p}_0\cdot\boldsymbol{v} - |M_0|^2\int\frac{d\mathbf{q}}{(2\pi)^2}\frac{|\rho(\mathbf{q})|^2}{q}\frac{1}{\omega_0 - \mathbf{q}\cdot\boldsymbol{v}}, \tag{55}$$

where $\rho(\mathbf{q}) = \langle\Psi|e^{i\mathbf{q}\cdot\mathbf{r}}|\Psi\rangle$. Equation (55) is minimized with respect to $\mathbf{p}_0$ by setting $\mathbf{p}_0 = m\boldsymbol{v}$ and, by expanding the last term of Eq. (55) up to the second order in $\boldsymbol{v}$, the corresponding minimum $J_v[\Psi]$ becomes[42]

$$J_v[\Psi] = E[\Psi] - \frac{m}{2}v^2\left[1 + \frac{2|M_0|^2}{m\omega_0^3}\int\frac{d\mathbf{q}}{(2\pi)^2}\frac{(\mathbf{q}\cdot\hat{\mathbf{u}})^2}{q}|\rho(\mathbf{q})|^2\right], \tag{56}$$

where $E[\Psi]$ is given in Eq. (30). From the above expression, it is clear that $J_v[\Psi]$ differs from $J_0[\Psi]$ at least to order v^2. Hence, if Ψ_v and Ψ_0 are the wave functions which minimize $J_v[\Psi]$ and $J_0[\Psi]$, respectively, then the difference $\Psi_v - \Psi_0$ is also of order v^2. As a consequence, the minimum of Eq.

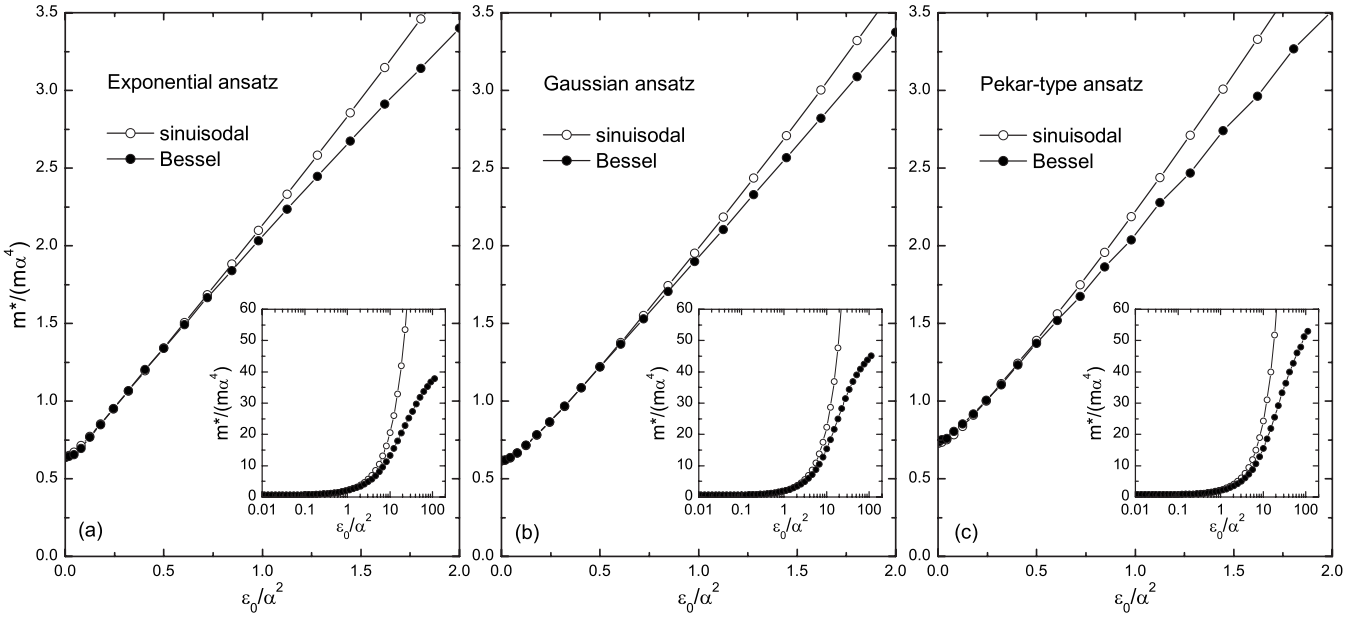

FIG. 4. Polaron mass enhancement m^*/m in units of α^4 as a function of ε_0/α^2 for different *Ansatz* wave functions. (a) Exponential, (b) Gaussian, (c) Pekar. Inset: $m^*/m\alpha^4$ is plotted for a wider range of SO values.

(56), $J_v[\Psi_v]$, differs from $J_v[\Psi_0]$ only to order $(\Psi_v-\Psi_0)^2=O(v^4)$ so that, by neglecting terms of higher order than v^2, minimization of Eq. (56) is achieved by the best wave function which minimizes $E[\Psi]$. Therefore, by using $E[\Psi_0]=E_P-E_0$ and evaluating $\langle\Psi_0|\mathbf{P}|\Psi_0\rangle$, from Eqs. (52) and (56) it turns out that

$$E_P(v)=E_P+\frac{m}{2}v^2\left[1+\frac{2|M_0|^2}{m\omega_0^3}\int\frac{d\mathbf{q}}{(2\pi)^2}\frac{(\mathbf{q}\cdot\hat{\mathbf{u}})^2}{q}|\rho_0(\mathbf{q})|^2\right], \tag{57}$$

permitting us to identify the quantity within square brackets as the mass enhancement factor m^*/m. By integrating over the direction of $\mathbf{q}$ and by using Eq. (5), m^*/m becomes in the strong-coupling limit

$$\frac{m^*}{m}=\frac{\sqrt{2}\pi\alpha}{(m\omega_0)^{3/2}}\int_0^\infty\frac{dq}{2\pi}q^2|\langle\Psi_0|e^{i\mathbf{q}\cdot\mathbf{r}}|\Psi_0\rangle|^2, \tag{58}$$

which, by replacing the momentum variable by the dimensionless quantity $\tilde{q}=ql_P$, gives a mass enhancement proportional to α^4 in the zero SO case. By using the exponential, Gaussian, and Pekar-type *Ansätze* in Eq. (58), the resulting mass enhancement factor becomes $m^*/m=(3/16)^3\pi^4\alpha^4\simeq 0.6421\alpha^4$, $m^*/m=(\pi/4)^2\alpha^4\simeq 0.617\alpha^4$, and $m^*/m\simeq 0.73\alpha^4$, respectively.[45]

The results for nonzero SO coupling are plotted in Fig. 4 for the sinuisodal (open circles) and Bessel (filled circles) spinors evaluated with exponential (a), Gaussian (b), and Pekar-type (c) wave functions. For all cases, m^*/m increases with ε_0/α^2 without much quantitative differences between the various *Ansätze* as long as $\varepsilon_0/\alpha^2\lesssim 2$. As shown in the insets of Fig. 4, for larger values of the SO coupling the use of the sinuisodal spinor largely overestimates the increase of the effective mass compared to the Bessel-type spinor results. However, despite of the weaker enhancement of m^*/m, the Bessel-type spinors give nevertheless an infinite effective mass at $\varepsilon_0/\alpha^2=\infty$. Indeed, independently of the particular form of $f(r)$, for $\varepsilon_0/\alpha^2\to\infty$ the expectation value $\langle\Psi_0|e^{i\mathbf{q}\cdot\mathbf{r}}|\Psi_0\rangle$ appearing in Eq. (58) goes like a/q for $q\to\infty$, rendering the integral over $q$of Eq. (58) divergent.

IV. DISCUSSION AND CONCLUSIONS

The results presented in the previous sections consistently show that, for both the weak and strong-coupling limits of the el-ph interaction, the ground-state energy E_P of the Fröhlich-Rashba polaron is lowered by the SO interaction and the mass is enhanced, leading to the conclusion that the Rashba coupling amplifies the polaronic character. This scenario suggests also that a weak-coupling polaron at $\varepsilon_0=0$ may be turned into a strong-coupling one for $\varepsilon_0>0$ or, more generally, that the crossover between weakly and strongly coupled polarons may be shifted by the SO interaction. This possibility can be tested by looking at the curves plotted in the main panel of Fig. 5, where the weak- and strong-coupling results for E_P/ω_0 are reported as a function of the el-ph coupling α for different ε_0 values. For $\varepsilon_0=0$, the polaron energy follows $E_P/\omega_0\simeq-\pi\alpha/2$ for small α and $E_P/\omega_0\simeq-0.4046\alpha^2$ for large α. These two limiting behaviors are plotted in Fig. 5 by the uppermost curves and compared with a numerical solutions of the Feynman variational path integral for the 2D polaron (filled circles). The largest deviation of the path integral solutions from the weak and strong-coupling approximations falls in the range of intermediate values of α and signals a region of crossover between the weakly and strongly coupled polaron. A rough estimate of the crossover position is given by a "critical" coupling, say α^*, obtained by equating the weak- and strong-coupling

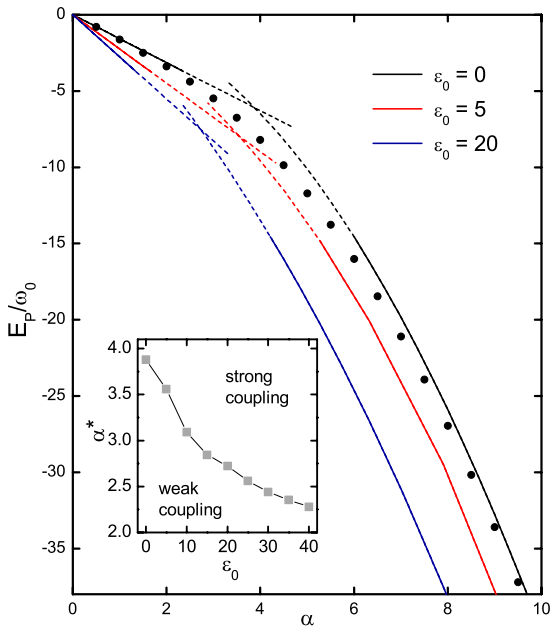

FIG. 5. (Color online) Ground-state polaron energy E_P as a function of the el-ph coupling α for different values of the dimensionless SO parameter $\varepsilon_0 = E_0/\omega_0$. The straight lines at small α refer to the weak-coupling results, while the curves at large α are the solution of the strong-coupling theory. The filled circles are the solution of the Feynman path integral *Ansatz* (see text). The point of intersection between the weak and strong-coupling curves is a measure of the crossover el-ph coupling α^*. Inset: α^* is plotted as a function of ε_0.

results. For $\varepsilon_0 = 0$ therefore one has $\pi\alpha/2 = 0.4046\alpha^2$, which gives $\alpha^* \simeq 3.9$. Now, as shown in Fig. 5 for $\varepsilon_0 = 5$ and $\varepsilon_0 = 20$, the increase of the SO interaction systematically reduces, for fixed α, the polaron ground-state energy and, at the same time, shifts the intersection point between the weak- and strong-coupling curves towards smaller values of the el-ph interaction. The "critical" value α^* of the crossover is therefore reduced by the SO interaction. For $\varepsilon_0 = 5$ and $\varepsilon_0 = 20$ it is found that $\alpha^* \simeq 3.6$ and $\alpha^* \simeq 2.7$, respectively. The systematic reduction of the crossover coupling by the SO interaction is made evident in the inset of Fig. 5, where α^* is plotted as a function of ε_0. From Fig. 5 it is also expected that, beside the reduction of α^*, the crossover region is likely to be narrowed by ε_0. Indeed, the intersection between the weak and strong coupling solutions for $\varepsilon_0 = 20$ is apparently smoother than the case for $\varepsilon_0 = 0$, suggesting that the true ground-state energy would deviate less, and in a narrower region around α^*, from the weak and strong-coupling solutions.

The scenario illustrated above, and in particular the SO effect on the crossover coupling, may be verified by quantum Monte-Carlo calculations of the Fröhlich-Rashba action or, more simply, by generalizing the Feynman *Ansatz* for the retarded interaction to $\varepsilon_0 > 0$.[7] The results presented here on the limiting cases $\alpha \ll 1$ and $\alpha \gg 1$ may then serve as a reference for such more general calculations schemes for arbitrary values of the el-ph coupling and of the SO interaction.

Let us discuss, before concluding, possible generalizations of the Fröhlich-Rashba model employed here and the consequences on the polaronic character. Let us remind the reader that in Ref. 31 it has been demonstrated that also for a momentum independent el-ph interaction model, the Rashba SO term leads to an effective enhancement of the el-ph coupling. The SO induced lowering of the polaron ground state is therefore robust against the specific form of the el-ph interaction, so that a similar behavior is expected to occur also when considering the contributions from interface or surface phonon modes. However, a different form of the SO interaction term may lead to a much weaker effect. Consider for example the situation in which, in addition to the Rashba SO coupling, the system lacks also of bulk inversion symmetry, as in III-V semiconductor heterostructures, leading to an extra SO term of the Dresselhaus type.[18,46] When both SO contributions are present, the square root divergence of the DOS at the bottom of the band of the free electron disappears, and it is replaced by a weaker logarithmic divergence at higher energies. In this situation therefore, at least for weak el-ph couplings, the SO interaction is expected to have a weaker effect on the polaron ground state, which tends to vanish as the Dresselhaus term becomes comparable to the Rashba one.

Let us conclude by noticing that, recently, the possibility of varying the coupling of 2D Fröhlich polarons in a controlled way has been experimentally demonstrated by acting on the dielectric polarizability of organic field-effect transistors.[47] The results presented here suggest that tunable 2D Fröhlich polarons may be achieved also by acting on the SO coupling, which can be tuned by applied gate voltages in quasi-2D structured materials.

ACKNOWLEDGMENTS

The author thanks Emmanuele Cappelluti and Frank Marsiglio for valuable comments.

[1] H. Fröhlich, Adv. Phys. **3**, 325 (1954).
[2] T. K. Mitra, A. Chatterjee, and S. Mukhopadhyay, Phys. Rep. **153**, 91 (1987).
[3] H. Fröhlich, H. Pelzer, and S. Zienau, Philos. Mag. **41**, 221 (1950).
[4] T. D. Lee, F. Low, and D. Pines, Phys. Rev. **90**, 297 (1953).
[5] S. I. Pekar, Zh. Eksp. Teor. Fiz. **16**, 355 (1946); **16**, 341 (1946).
[6] S. J. Miyake, J. Phys. Soc. Jpn. **38**, 181 (1975); **41**, 747 (1976).
[7] R. P. Feynman, Phys. Rev. **97**, 660 (1955).
[8] G. Ganbold and G. V. Efimov, Phys. Rev. B **50**, 3733 (1994); J. Phys.: Condens. Matter **10**, 4845 (1998).
[9] G. De Filippis, V. Cataudella, V. Marigliano Ramaglia, C. A. Perroni, and D. Bercioux, Eur. Phys. J. B **36**, 65 (2003).
[10] C. Alexandrou, W. Fleischer, and R. Rosenfelder, Phys. Rev. Lett.

65, 2615 (1990).
[11] J. T. Titantah, C. Pierleoni, and S. Ciuchi, Phys. Rev. Lett. **87**, 206406 (2001).
[12] S. Das Sarma and B. A. Mason, Ann. Phys. (N.Y.) **163**, 78 (1985).
[13] W. J. Huybrechts, Solid State Commun. **28**, 95 (1978).
[14] Xiaoguang Wu, F. M. Peeters, and J. T. Devreese, Phys. Rev. B **31**, 3420 (1985).
[15] F. M. Peeters, X. Wu, and J. T. Devreese, Phys. Rev. B **37**, 933 (1988).
[16] C. Qinghu, F. Minghu, Z. Qirui, W. Kelin, and W. Shaolong, J. Phys.: Condens. Matter **8**, 7139 (1996).
[17] J. T. Devreese, J. Phys.: Condens. Matter **19**, 255201 (2007).
[18] I. Žutić, J. Fabian, and S. Das Sarma, Rev. Mod. Phys. **76**, 323 (2004).
[19] S. LaShell, B. A. McDougall, and E. Jensen, Phys. Rev. Lett. **77**, 3419 (1996).
[20] Yu. M. Koroteev, G. Bihlmayer, J. E. Gayone, E. V. Chulkov, S. Blugel, P. M. Echenique, and P. Hofmann, Phys. Rev. Lett. **93**, 046403 (2004).
[21] K. Sugawara, T. Sato, S. Souma, T. Takahashi, M. Arai, and T. Sasaki, Phys. Rev. Lett. **96**, 046411 (2006).
[22] E. Rotenberg, J. W. Chung, and S. D. Kevan, Phys. Rev. Lett. **82**, 4066 (1999).
[23] D. Pacilé, C. R. Ast, M. Papagno, C. Da Silva, L. Moreschini, M. Falub, Ari. P. Seitsonen, and M. Grioni, Phys. Rev. B **73**, 245429 (2006).
[24] C. R. Ast, G. Wittich, P. Wahl, R. Vogelgesang, D. Pacilé, M. C. Falub, L. Moreschini, M. Papagno, M. Grioni, and K. Kern, Phys. Rev. B **75**, 201401(R) (2007).
[25] C. R. Ast, J. Henk, A. Ernst, L. Moreschini, M. C. Falub, D. Pacilé, P. Bruno, K. Kern, and M. Grioni, Phys. Rev. Lett. **98**, 186807 (2007).
[26] I. I. Boiko and E. I. Rashba, Sov. Phys. Solid State **2**, 1692 (1960).
[27] A. G. Galstyan and M. E. Raikh, Phys. Rev. B **58**, 6736 (1998).
[28] C. Grimaldi, Phys. Rev. B **72**, 075307 (2005).
[29] A. V. Chaplik and L. I. Magarill, Phys. Rev. Lett. **96**, 126402 (2006); Photonics Spectra **34**, 344 (2006).
[30] E. Cappelluti, C. Grimaldi, and F. Marsiglio, Phys. Rev. Lett. **98**, 167002 (2007).
[31] E. Cappelluti, C. Grimaldi, and F. Marsiglio, Phys. Rev. B **76**, 085334 (2007).
[32] E. Evans and D. L. Mills, Phys. Rev. B **8**, 4004 (1973); H. Sun and S. -W. Gu, Phys. Rev. B **40**, 11576 (1989).
[33] The form of the self-energy reported in Eq. (12) is not limited to the weak-coupling limit. For a more general derivation see Ref. 31.
[34] There are however quantitative differences. Indeed, in the strong SO limit, the Holstein-Rashba model gives an effective mass enhancement proportional to $\sqrt{\varepsilon_0}$, i.e., a weaker increase with respect to the linear dependence found here for the Fröhlich-Rashba model (see Ref. 31).
[35] J. Liu and J. -L. Xiao, Commun. Theor. Phys. **46**, 761 (2006).
[36] Z. Li, Z. Ma, A. R. Wright, and C. Zhang, Appl. Phys. Lett. **90**, 112103 (2007).
[37] The term "trapping" is used here in a loose way, since no real trapping effect exist for the continuum Fröhlich polaron.
[38] M. Donsker and S. R. S. Varadhan, Commun. Pure Appl. Math. **36**, 505 (1983).
[39] E. H. Lieb and L. E. Thomas, Commun. Math. Phys. **183**, 511 (1997).
[40] E. N. Bulgakov and A. F. Sadreev, JETP Lett. **73**, 505 (2001).
[41] E. Tsitsishvili, G. S. Lozano, and A. O. Gogolin, Phys. Rev. B **70**, 115316 (2004).
[42] G. R. Allcock, Adv. Phys. **5**, 412 (1956).
[43] R. Parker, G. Whitfield, and M. Rona, Phys. Rev. B **10**, 698 (1974).
[44] J. da Providencia, M. da Conceição Ruivo, and C. A. de Sousa, Ann. Phys. (N.Y.) **91**, 366 (1975).
[45] Note that the result for the exponential *Ansatz* differs from that of Ref. 15. The difference stems from an incorrect expression of the exponential decay factor a: in Ref. 15 $a/l_P=3\pi/8$ while instead it should be given by $a/l_P=3\pi/16$, as in Ref. 14 and in the present paper.
[46] G. Dresselhaus, Phys. Rev. **100**, 580 (1955).
[47] I. N. Hulea, S. Fratini, H. Xie, C. L. Mulder, N. N. Iossad, G. Rastelli, S. Ciuchi, and A. F. Morpurgo, Nat. Mater. **5**, 982 (2006).